

# The *ab initio* simulation of the Earth's core

BY D. ALFÉ<sup>1,2</sup>, M. J. GILLAN<sup>2</sup>, L. VOČADLO<sup>1</sup>,  
J. BRODHOLT<sup>1</sup> AND G. D. PRICE<sup>1</sup>

<sup>1</sup>*Research School of Geological and Geophysical Sciences, Birkbeck and University College London, Gower Street, London WC1E 6BT, UK*

<sup>2</sup>*Department of Physics and Astronomy, University College London, Gower Street, London WC1E 6BT, UK*

*Published online 25 April 2002*

The Earth has a liquid outer and solid inner core. It is predominantly composed of Fe, alloyed with small amounts of light elements, such as S, O and Si. The detailed chemical and thermal structure of the core is poorly constrained, and it is difficult to perform experiments to establish the properties of core-forming phases at the pressures (*ca.* 300 GPa) and temperatures (*ca.* 5000–6000 K) to be found in the core. Here we present some major advances that have been made in using quantum mechanical methods to simulate the high-*P/T* properties of Fe alloys, which have been made possible by recent developments in high-performance computing. Specifically, we outline how we have calculated the Gibbs free energies of the crystalline and liquid forms of Fe alloys, and so conclude that the inner core of the Earth is composed of hexagonal close packed Fe containing *ca.* 8.5% S (or Si) and 0.2% O in equilibrium at 5600 K at the boundary between the inner and outer cores with a liquid Fe containing *ca.* 10% S (or Si) and 8% O.

**Keywords:** Earth's core; iron; *ab initio*; molecular dynamics; computational mineral physics

## 1. Introduction

The Earth's core is the seat of major global processes: convection in the core generates the Earth's magnetic field, while heat flow from the core contributes significantly to driving mantle convection and hence ultimately contributes to plate tectonics and the resulting earthquake and volcanic activity. To understand core processes, it is necessary to know the physical properties of core-forming materials. From seismology, we know that the core lies at a depth of *ca.* 2890 km beneath the Earth's surface, that the liquid outer core extends to a depth of *ca.* 5150 km, and that the inner core beneath it is crystalline (figure 1). On the basis of materials-density/sound-wave velocity systematics (figure 2), Birch (1964) concluded that the core is composed of iron alloyed with a small fraction of lighter elements. Today we believe that the outer core is *ca.* 6–10% less dense than pure liquid Fe, while the inner core solid is a few per cent less dense than Fe (Poirier 1994). It is generally held that the inner core is crystallizing from the outer core as the Earth slowly cools, and that core temperatures are in the range 4000–7000 K, while the pressure at the centre of the

One contribution of 15 to a Discussion Meeting 'New science from high-performance computing'.

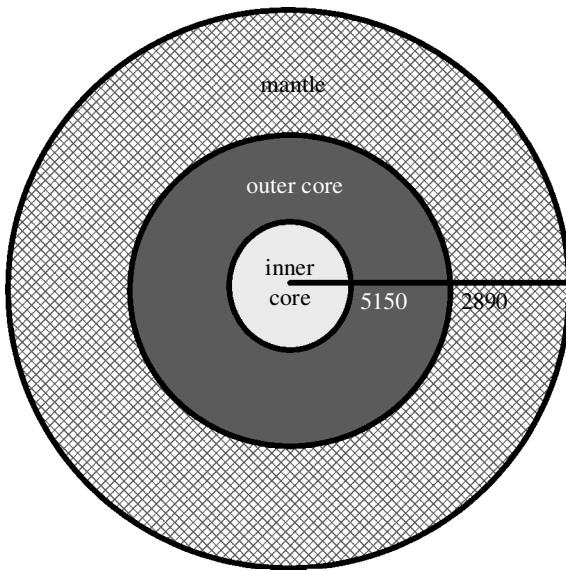


Figure 1. Schematic cross-section of the Earth showing the core–mantle boundary at a depth of 2890 km and the boundary between the inner and outer cores at a depth of 5150 km.

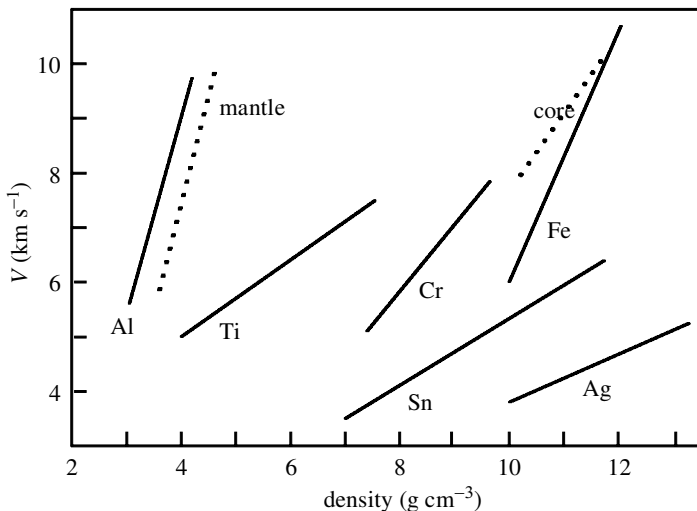


Figure 2. Schematic of the bulk sound velocity versus specific mass of some metals, from shock-wave data (solid lines). The dashed curves for the mantle and core obtained from seismic data are also shown (after Birch 1964).

Earth is *ca.* 360 GPa. The exact temperature profile and composition of the core are unknown, but from cosmochemical and other considerations, it has been suggested (Poirier 1994) that the alloying elements in the core might include S, O, Si, H and C. It is also possible that the core contains small amounts of other elements, such as Ni and K.

In order to develop a more accurate description of the behaviour of the core and the evolution of our planet, it is necessary to determine in greater detail the physical

properties and phase relations of the Fe system at the conditions relevant to the core. Experimental techniques have evolved rapidly in the past few years, and today, using diamond anvil cells or shock experiments, the study of minerals at pressures up to *ca.* 200 GPa and temperatures of a few thousand kelvin is possible. These studies, however, are still far from routine and results from different groups are often in conflict. As a result, therefore, in order to complement these existing experimental studies and to extend the range of pressure and temperature over which we can model the Earth, computational mineral physics has, in the past decade, become an established and growing discipline.

The aims of computational mineral physics are twofold: (i) to provide an atomistic underpinning to existing experimental data, and (ii) to provide a sound basis upon which to extrapolate beyond the limitations of current experimental methods. In order to achieve these aims, a variety of atomistic simulation methods (developed originally in the fields of solid-state physics and theoretical chemistry) are used. These techniques can be divided approximately into those that use some form of interatomic potential model to describe the energy of the interaction of atoms in a mineral as a function of atomic separation and geometry, and those that involve the solution of Schrödinger's equation to calculate the energy of the mineral species by quantum mechanical techniques. For the Earth sciences, the accurate description of the behaviour of minerals as a function of temperature is particularly important, and computational mineral physics usually uses either statistical mechanical methods (based upon lattice dynamics) or molecular dynamics methods to achieve this important step. The relatively recent application of all of these methods to geophysics has only been possible because of the very rapid advances in the power and speed of computer processors. Techniques which in the past were limited to the study of structurally simple compounds, with small unit cells, can today be applied to describe the behaviour of the complex, low-symmetry structures (which epitomize most minerals) and liquids.

In this paper, we will focus on our recent studies of Fe and its alloys, which have been aimed at predicting their geophysical properties and behaviour under core conditions. Although interatomic potentials can be used to study many mineral properties, metallic phases such as Fe are best modelled by quantum mechanical methods, so below we outline the essential *ab initio* techniques used in our studies. We then present our predictions of the structure of the stable phase of Fe at core pressures and temperatures, its melting behaviour at core pressures, and an *ab initio* estimate of the composition and temperature of the inner and outer core.

## 2. Quantum mechanical simulations

*Ab initio* simulations are based on the description of the electrons within a system in terms of a quantum mechanical wave function,  $\psi$ , the energy and dynamics of which is governed by the general Schrödinger equation for a non-relativistic single particle in free space of mass  $m$ :

$$i\hbar \frac{\partial \psi}{\partial t} = -\frac{\hbar^2}{2m} \nabla^2 \psi. \quad (2.1)$$

However, in minerals, the electrons are confined within a crystal, and there is a perturbation to the energy associated with this bound system,  $V(r)$ , and the Schrödinger

equation may then be written for a single bound electron:

$$i\hbar \frac{\partial \psi}{\partial t} = -\frac{\hbar^2}{2m} \nabla^2 \psi + V(r)\psi. \quad (2.2)$$

In this case, the electron, no longer in free space, is repeatedly and infinitely scattered within the crystal, so the solution to the Schrödinger equation is either one of a multiple-scatter problem, or alternatively the eigenstates (stationary states) of the electrons in the lattice may be obtained. In minerals, however, it is necessary to take into account all the electrons within the crystal, so the energy,  $E$ , of a many-electron wave function,  $\Psi$ , is required:

$$E\Psi(r_1, r_2, \dots, r_N) = \left( \sum -\frac{\hbar^2}{2m} \nabla^2 + V_{\text{ion}} + V_{\text{e-e}} \right) \Psi(r_1, r_2, \dots, r_N). \quad (2.3)$$

In a confined system, the electrons experience interactions between the nuclei and each other. This perturbation to the energy of the electron in free space may be expressed in terms of an ionic contribution and a Coulombic contribution (the second and third terms within the brackets); the total energy is that summed over all wave functions, and energy minimization techniques may then be applied in order to obtain the equilibrium structure for the system under consideration.

Unfortunately, the complexity of the wave function,  $\Psi$ , for an  $N$ -electron system scales as  $M^N$ , where  $M$  is the number of degrees of freedom for a single-electron wave function,  $\psi$ . This type of problem cannot readily be solved for large systems due to computational limitations, and therefore the exact solution to the problem for large systems is intractable. However, there are a number of approximations that may be made to simplify the calculation, whereby good predictions of the structural and electronic properties of materials can be obtained by solving self-consistently the one-electron Schrödinger equation for the system, and then summing these individual contributions over all the electrons in the system (for a general review, see Gillan (1997)). Such approximation techniques include the Hartree–Fock approximation (HFA) and density functional theory (DFT), which differ in their description of the electron–electron interactions. In both cases the average electrostatic field surrounding each electron is treated similarly, reducing the many body Hamiltonian in the Schrödinger equation for a non-spin-polarized system to that for one electron surrounded by an effective potential associated with the interactions of the surrounding crystal; however, the difference between the two methods arises in the treatment of the contribution to the potential associated with the fact that the electron is not in a average field, the correlation, and also in the treatment of the electronic spin governed by Pauli's exclusion principle, the exchange. In the HFA the exchange interactions are treated exactly, but the correlation is not included; in modern geophysical studies, the DFT is increasingly favoured, where the exchange and correlation are both included, but only in an average way.

DFT, originally developed by Hohenberg & Kohn (1964) and Kohn & Sham (1965), describes the exact ground-state properties of a system in terms of a unique functional of charge density alone, i.e.  $E = E(\rho)$ . The Hohenberg–Kohn theorem says that the ground-state density uniquely determines the potential (and so all the physical properties of the system). Using the variational principle it is easy to show that the ground-state density minimizes the total energy. So by looking for the minimum of

the total energy, we find the ground-state density. In DFT, the electronic energy may be written as follows:

$$E_{\text{electronic}} = \int V_{\text{ion}}(r)\rho(r) d^3r + E_{\text{Electrostatic}} + E_{\text{xc}}[\rho]. \quad (2.4)$$

Therefore, by varying the electron density of the system through a search of single-particle density space until the minimum energy configuration is found, an exact ground-state energy is achieved, and that electron density is the exact ground-state energy for the system; all other ground-state properties are functions of this ground-state electron density. However, the exact form of the functional  $E_{\text{xc}}[\rho]$  is not known, and is approximated by a local function of the density. This local density approximation (LDA) defines the exchange-correlation potential as a function of electron density at a given coordinate position (Kohn & Sham 1965). Sometimes it is a better approximation to use the generalized gradient approximation (GGA) (Wang & Perdew 1991), which has a similar form for the exchange-correlation potential, but has it as a function of both the local electron density and the magnitude of its gradient. The shortcomings of these approximations when applied to oxide and metallic phases do not seem to be great, but in the future they might be avoided by using techniques such as quantum Monte Carlo, which will, however, demand even greater computing resources.

In our simulations, the electronic wave functions are expanded in a plane-wave basis set, with the electron-ion interactions described by means of ultra-soft Vanderbilt pseudo-potentials (PPs). A PP is a modified form of the true potential experienced by the electrons (Heine 1970; Cohen & Heine 1970; Heine & Weaire 1970). When they are near the nucleus, the electrons feel a strong attractive potential and this gives them a high kinetic energy. But this means that their de Broglie wavelength is very small, and their wavevector is very large. Because of this, a plane-wave basis would have to contain so many wavevectors that the calculations would become very demanding. So-called 'all-electron' calculations are possible, but generally they have been limited to small systems. A remarkable way of eliminating this problem and broadening the range of systems that can be studied was developed by Heine, Cohen and others, who showed that it is possible to represent the interaction of the valence electrons with the atomic cores by a weak effective 'pseudo-potential' and still end up with a correct description of the electron states and the energy of the system. In this way of doing it, the core electrons are assumed to be in exactly the same states that they occupy in the isolated atom, which is usually valid.

Plane waves have proved to be very successful for many reasons. The wave functions can be made as accurate as necessary by increasing the number of plane waves, so that the method is systematically improvable. Plane waves are simple so that the programming is easy, and it also turns out that the forces on the ions are straightforward to calculate, so that it is easy to move them. Finally, plane waves are unbiased. The calculations are unaffected by the prejudices of the user—an important advantage for any method that is going to be widely used. As such using GGA within DFT combined with PPs provides an excellent technique with which to accurately explore crystal structures. However, for our studies, we need not only to explore the energetics of the bonding in a crystal, but we are also concerned with the effect of temperature on the system. This requires us to calculate the Gibbs free energy of the systems, which can be done either using lattice dynamic or molecular dynamic methods.

## (a) Lattice dynamics

The lattice dynamics method is a semi-classical approach that uses the quasi-harmonic approximation (QHA) to describe a cell in terms of independent quantized harmonic oscillators whose frequencies vary with cell volume, thus allowing for a description of thermal expansion (Born & Huang 1954). The motions of the individual particles are treated collectively as lattice vibrations or phonons, and the phonon frequencies,  $\omega(q)$ , are obtained by solving

$$m\omega^2(q)e_i(q) = D(q)e_j(q), \quad (2.5)$$

where  $m$  is the mass of the atom, and the dynamical matrix,  $D(q)$ , is defined by

$$D(q) = \sum_{ij} \left( \frac{\partial^2 U}{\partial u_i \partial u_j} \right) \exp(iq \cdot r_{ij}), \quad (2.6)$$

where  $r_{ij}$  is the interatomic separation and  $u_i$  and  $u_j$  are the atomic displacements from their equilibrium position. For a unit cell containing  $N$  atoms, there are  $3N$  eigenvalue solutions ( $\omega^2(q)$ ) for a given wave vector  $q$ . There are also  $3N$  sets of eigenvectors ( $e_x(q)$ ,  $e_y(q)$ ,  $e_z(q)$ ) which describe the pattern of atomic displacements for each normal mode.

The vibrational frequencies of a lattice can be calculated *ab initio*, by standard methods such as the small-displacement method (Kresse *et al.* 1995). Having calculated the vibrational frequencies, a number of thermodynamic properties may be calculated using standard statistical mechanical relations, which are direct functions of these vibrational frequencies. Thus for example the Helmholtz free energy is given by

$$F = k_B T \sum_i^M (\frac{1}{2}x + \ln(1 - e^{-x})), \quad (2.7)$$

where  $x_i = \hbar\omega_i/k_B T$ , and the sum is over all the  $M$  normal modes. Modelling the effect of pressure is essential if one is to obtain accurate predictions of phenomena such as phase transformations and anisotropic compression. This problem is now routinely being solved using codes that allow constant stress, variable geometry cells in both static and dynamic simulations. In the case of lattice dynamics, the mechanical pressure is calculated from strain derivatives, while the thermal kinetic pressure is calculated from phonon frequencies (Parker & Price 1989). The balance of these forces can be used to determine the variation of cell size as a function of pressure and temperature.

The QHA assumes that the lattice vibrational modes are independent. However, at high temperatures, where vibrational amplitudes become large, phonon–phonon scattering becomes important, and the QHA breaks down. Since, at ambient pressure, the QHA is only valid for  $T < \omega_D$ , the Debye temperature, if we are interested in the extreme conditions of the interior Earth, we would expect to have to modify this methodology to enable higher temperatures to be simulated (see, for example, Wallace 1998), alternatively we could use molecular dynamics techniques. Matsui *et al.* (1994) have shown, however, that the inherent anharmonicity associated with lattice dynamics decreases with increasing pressure, and the two techniques give very similar results for very-high-pressure and temperature simulations.

## (b) Molecular dynamics

Molecular dynamics (MD) is routinely used for medium- to high-temperature simulations of minerals, especially at lower pressures, where the QHA breaks down in lattice dynamics, and in the simulation of liquids, where lattice dynamics is of course inapplicable. The method is essentially classical, and is outlined in detail in Allen & Tildesley (1987). In principle Newton's equations of motion are solved for a number of particles within a simulation box to generate time-dependent trajectories and the associated positions and velocities which evolve with each time-step. Here the kinetic energy, and therefore temperature, is obtained directly from the velocities of the individual particles. With this explicit particle motion, the anharmonicity is implicitly accounted for at high temperatures.

The interactions between the atoms within the system have traditionally been described in terms of the interatomic potential models mentioned earlier, but instead of treating the atomic motions in terms of lattice vibrations, each ion is treated individually. As the system evolves, the required dynamic properties are calculated iteratively at the specified pressure and temperature. The ions are initially assigned positions and velocities within the simulation box; their coordinates are usually chosen to be at the crystallographically determined sites, while their velocities are equilibrated such that they concur with the required system temperature, and such that both energy and momentum is conserved. In order to calculate subsequent positions and velocities, the forces acting on any individual ion are then calculated from the first derivative of the potential function, and the new position and velocity of each ion may be calculated at each time-step by solving Newton's equation of motion. Both the particle positions and the volume of the system, or simulation box, can be used as dynamical variables, as is described in detail in Parrinello & Rahman (1980).

Because of advances in computer power, it is now possible to perform *ab initio* molecular dynamics (AIMD), with the forces calculated fully quantum mechanically (within the GGA and the PP approximations) instead of relying upon the use of interatomic potentials. The first pioneering work in AIMD was that of Car & Parrinello (1985), who proposed a unified scheme to calculate *ab initio* forces on the ions and keep the electrons close to the Born–Oppenheimer surface while the atoms move. We have used here an alternative approach, in which the dynamics are performed by explicitly minimizing the electronic free-energy functional at each time-step. This minimization is more expensive than a single Car–Parrinello step, but the cost of the step is compensated by the possibility of making longer time-steps. The MD simulations presented here have been performed using VASP (Vienna *ab initio* simulation package). In VASP the electronic ground state is calculated exactly (within a self-consistent threshold) at each MD step, using an efficient iterative matrix diagonalization scheme and the mixer scheme of Pulay (1980). We have also implemented a scheme to extrapolate the electronic charge density from one step to the next, with an efficiency improvement of about a factor of two (Alfè 1999). Since we are interested in finite-temperature simulations, the electronic levels are occupied according to the Fermi statistics corresponding to the temperature of the simulation. This prescription also avoids problems with level crossing during the self-consistent cycles. For more details of the VASP code see Kresse & Furthmüller (1996). Below, we illustrate our use of these methods in the study of Fe and its alloys at extreme pressure and temperature.

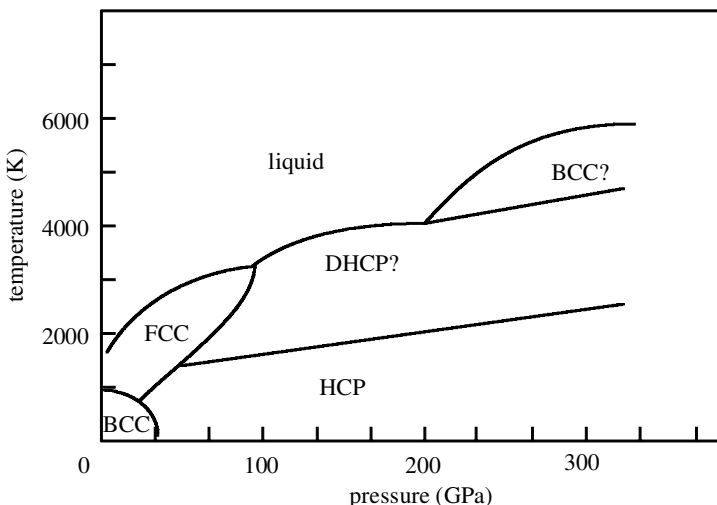


Figure 3. A hypothetical phase diagram for Fe, incorporating all the experimentally suggested high- $P/T$  phase transformations. Our calculations suggest that the phase diagram is in fact much more simple than this, with HCP-Fe being the only high- $P/T$  phase stable at core pressures.

### 3. The structure of Fe under core conditions

Under ambient conditions, Fe adopts a body-centred cubic (BCC) structure, that transforms with temperature to a face-centred cubic (FCC) form, and with pressure transforms to a hexagonal close-packed (HCP) phase,  $\varepsilon$ -Fe. The high- $P/T$  phase diagram of pure iron itself, however, is still controversial (see figure 3). Various diamond-anvil-based studies have suggested that HCP-Fe transforms at high temperatures to a phase which has variously been described as having a double hexagonal close-packed structure (DHCP) (Saxena *et al.* 1996) or an orthorhombic distortion of the HCP structure (Andrault *et al.* 1997). Furthermore, high-pressure shock experiments have also been interpreted as showing a high-pressure solid–solid phase transformation (Brown & McQueen 1986), which has been suggested could be due to the development of a BCC phase (Matsui & Anderson 1997). Other experimentalists, however, have failed to detect such a post-HCP phase (Shen *et al.* 1998; Nguyen & Holmes 1998, 2001), and have suggested that the previous observations were due either to minor impurities or to metastable strain-induced behaviour.

Further progress in interpreting the nature and evolution of the core would be severely hindered if the uncertainty concerning the crystal structure of the core's major chemical component remained unresolved. Such uncertainties can be resolved, however, using *ab initio* calculations, which we have shown provide an accurate means of calculating the thermoelastic properties of materials at high  $P$  and  $T$  (Vočadlo *et al.* 1999). Thermodynamic calculations on HCP-Fe and FCC-Fe at high  $P/T$  have already been reported (Stixrude *et al.* 1997; Wasserman *et al.* 1996) in which *ab initio* calculations were used to parametrize a tight-binding model; the thermal properties of this model were then obtained using the particle-in-a-cell method. The calculations that we performed (Vočadlo *et al.* 1999) to determine the high- $P/T$  structure of Fe using the Cray T3E at Edinburgh were the first in which fully *ab initio* methods were used in conjunction with quasi-harmonic lattice dynamics to obtain free energies of all the candidate structures proposed for core conditions.

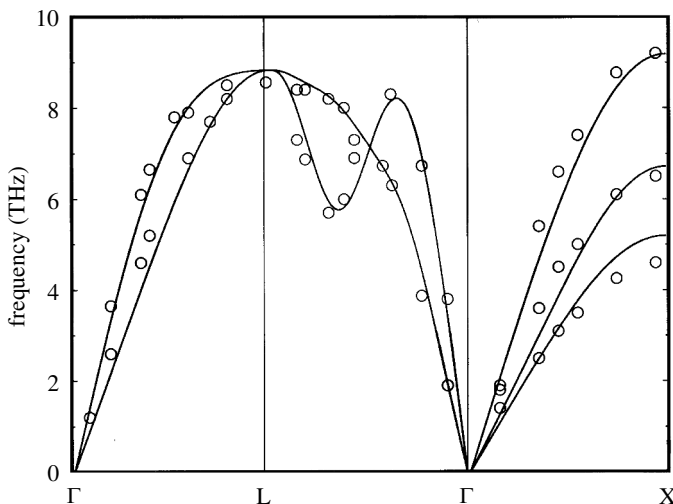


Figure 4. The phonon dispersion curves for BCC-Fe ( $T = 0$ ,  $P = 0$ ). The solid lines are from our calculations, and the open circles are experimental points reported in Gao *et al.* (1993).

Spin-polarized simulations were initially performed on a variety of candidate phases (including a variety of distorted BCC and HCP structures and the DHCP phase) at pressures ranging from 325 to 360 GPa. These revealed, in agreement with Söderlind *et al.* (1996), that under these conditions only BCC-Fe had a small residual magnetic moment and all other phases had zero magnetic moment. We found that at these pressures the BCC and the suggested orthorhombic polymorph of iron (Andrault *et al.* 1997) are mechanically unstable. The BCC phase continuously transforms to the FCC phase (confirming the findings of Stixrude & Cohen (1995)), while the orthorhombic phase spontaneously transforms to the HCP phase when allowed to relax to a state of isotropic stress. In contrast, HCP, DHCP and FCC-Fe remain mechanically stable at core pressures, and we were therefore able to calculate their phonon frequencies and free energies.

Although no experimentally determined phonon-dispersion curves exist for HCP-Fe, the quality of our calculations can be gauged by comparing the calculated phonon dispersion for BCC-Fe (done using fully spin-polarized calculations), at ambient pressure, where experimental data do exist. Figure 4 shows the phonon dispersion curve for magnetic BCC-Fe at ambient conditions compared with inelastic neutron scattering experiments (see Gao *et al.* 1993); the calculated frequencies are in excellent agreement with the experimental values. This further confirms the quality of the PP used in our study.

The thermal pressure at core conditions has been estimated to be 58 GPa (Anderson 1995) and 50 GPa (Stixrude *et al.* 1997); these are in excellent agreement with our calculated thermal pressure for the HCP and DHCP structures (58 GPa and 49 GPa, respectively, at 6000 K); however, our calculated thermal pressure is considerably higher for FCC-Fe, and we find that this thermodynamically destabilizes this phase at core conditions with respect to DHCP and HCP-Fe. By analysing the total pressure as a function of temperature obtained from our calculations for these two phases, we are able to ascertain the temperature as a function of volume at two pressures ( $P = 325$  GPa and  $P = 360$  GPa) that span the inner-core range

of pressures. From this we could determine the Gibbs free energy at those  $T$  and  $P$ . We found that over the whole  $P/T$  space investigated the HCP phase has the lower Gibbs free energy, and we therefore predict HCP–Fe to be the stable structure at core conditions. We suggest that some of complexity indicated by experiment is either confined to pressures lower than those in the core (i.e. *ca.* 100 GPa) or is strain-induced metastable behaviour.

#### 4. The high- $P$ melting of Fe

An accurate knowledge of the melting properties of iron is particularly important, as the temperature distribution in the core is relatively uncertain and a reliable estimate of the melting temperature of iron at the pressure of the inner-core boundary (ICB) would put a much-needed constraint on core temperatures. Static compression measurements of  $T_m$  with the diamond anvil cell (DAC) have been made up to *ca.* 200 GPa (Boehler 1993), but even at lower pressures results for  $T_m$  disagree by several hundred kelvin. Shock experiments are at present the only available method of  $T_m$  measurement at higher pressures, but their interpretation is not simple, and there is a scatter of at least 2000 K in  $T_m$  at ICB pressures (see Nguyen & Holmes 1998, 2002).

Since both our calculations and recent experiments (Shen *et al.* 1998) suggest that Fe melts from the  $\epsilon$ -phase in the pressure range immediately above 60 GPa, we focus here on equilibrium between HCP–Fe and liquid phases. The condition for two phases to be in thermal equilibrium at a given temperature,  $T$ , and pressure,  $P$ , is that their Gibbs free energies,  $G(P, T)$ , are equal. To determine  $T_m$  at any pressure, we calculate  $G$  for the solid and liquid phases as a function of  $T$  and determine where they are equal. In fact, we calculate the Helmholtz free energy,  $F(V, T)$ , as a function of volume,  $V$ , and hence obtain the pressure through the relation  $P = -(\partial F / \partial V)_T$  and  $G$  through its definition  $G = F + PV$ .

To obtain melting properties with useful accuracy, free energies must be calculated with high precision, because the free-energy curves for liquid and solid cross at a shallow angle. It can readily be shown that to obtain  $T_m$  with a technical precision of 100 K, non-cancelling errors in  $G$  must be reduced below 10 meV. Errors in the rigid-lattice free energy due to basis-set incompleteness and Brillouin-zone sampling are readily reduced to a few meV per atom. In this study, the lattice vibrational frequencies were obtained by diagonalizing the force-constant matrix; this matrix was calculated by our implementation of the small-displacement method described by Kresse *et al.* (1995). The difficulty in calculating the harmonic free energy is that frequencies must be accurately converged over the whole Brillouin zone. This requires that the free energy is fully converged with respect to the range of the force-constant matrix. To attain the necessary precision we used repeating cells containing 36 atoms, and to show that such cells surface we performed some highly computationally demanding calculations on cells of up to 150 atoms.

To calculate the liquid free energy and the anharmonic contribution to the solid free energy, we use the technique of ‘thermodynamic integration’, which yields the difference between the free energy ( $\Delta F$ ) of the *ab initio* system and that of a reference system. The basis of the technique (see, for example, de Wijs *et al.* 1998) is that  $\Delta F$  is the work done on reversibly and isothermally switching from the reference total-energy function,  $U_{\text{ref}}$ , to the *ab initio* total energy,  $U$ . This switching is done

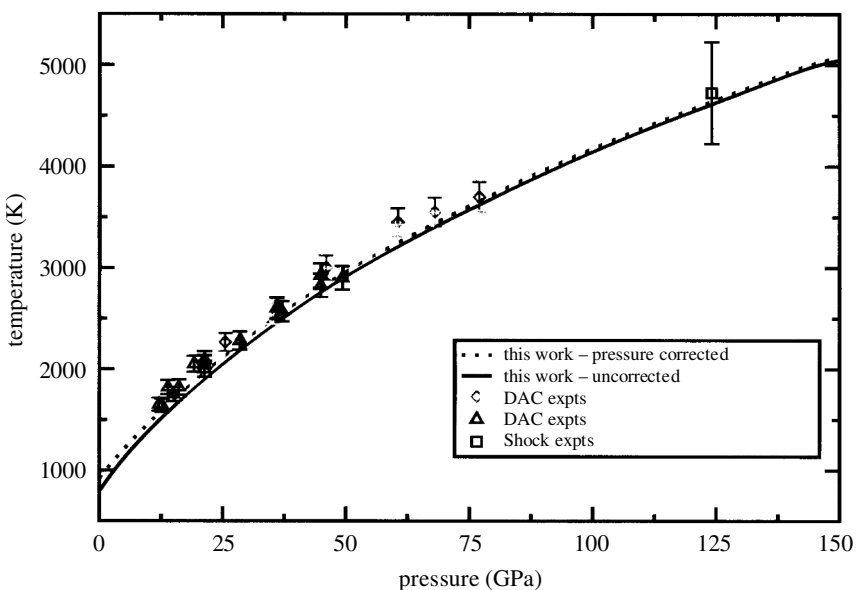


Figure 5. Our calculated high-pressure melting curve for Al (see Vočadlo & Alfè 2002) is shown passing through a variety of recent high- $P$  experimental points.

by passing through intermediate total-energy functions  $U_\lambda$  given by

$$U_\lambda = (1 - \lambda)U_{\text{ref}} + \lambda U.$$

It is a standard result that the work done is

$$\Delta F = \int_0^1 d\lambda \langle U - U_{\text{ref}} \rangle_\lambda, \quad (4.1)$$

where the thermal average  $\langle U - U_{\text{ref}} \rangle_\lambda$  is evaluated for the system governed by  $U_\lambda$ . The practical feasibility of calculating *ab initio* free energies of liquids and anharmonic solids depends on finding a reference system for which  $F_{\text{ref}}$  is readily calculable and the difference  $(U - U_{\text{ref}})$  is very small. In our studies of liquid Fe, the primary reference state chosen was an inverse power potential. The full technical details involved in our calculations are given in Alfè *et al.* (2002).

To confirm that the methodology can be used accurately to calculate melting temperatures, we modelled the well-studied high- $P$  melting behaviour of Al (de Wijs *et al.* 1998; Vočadlo & Alfè 2002). Figure 5 shows the excellent agreement that we obtained for this system. In 1999 we published an *ab initio* melting curve for Fe (Alfè *et al.* 1999). Since the work reported in that paper, we have improved our description of the *ab initio* free energy of the solid, and have revised our estimate of  $T_m$  of Fe at ICB pressures to be between 6200 and 6350 K (see figure 6). For pressures  $P < 200$  GPa (the range covered by DAC experiments) our curve lies *ca.* 900 K above the values of Boehler (1993) and *ca.* 200 K above the more recent values of Shen *et al.* (1998) (who stress that their values are only a lower bound to  $T_m$ ). Our curve falls significantly below the shock-based estimates for the  $T_m$  of Yoo *et al.* (1993) in which temperature was deduced by measuring optical emission (however, the difficulties of obtaining temperature by this method in shock experiments are well known), but

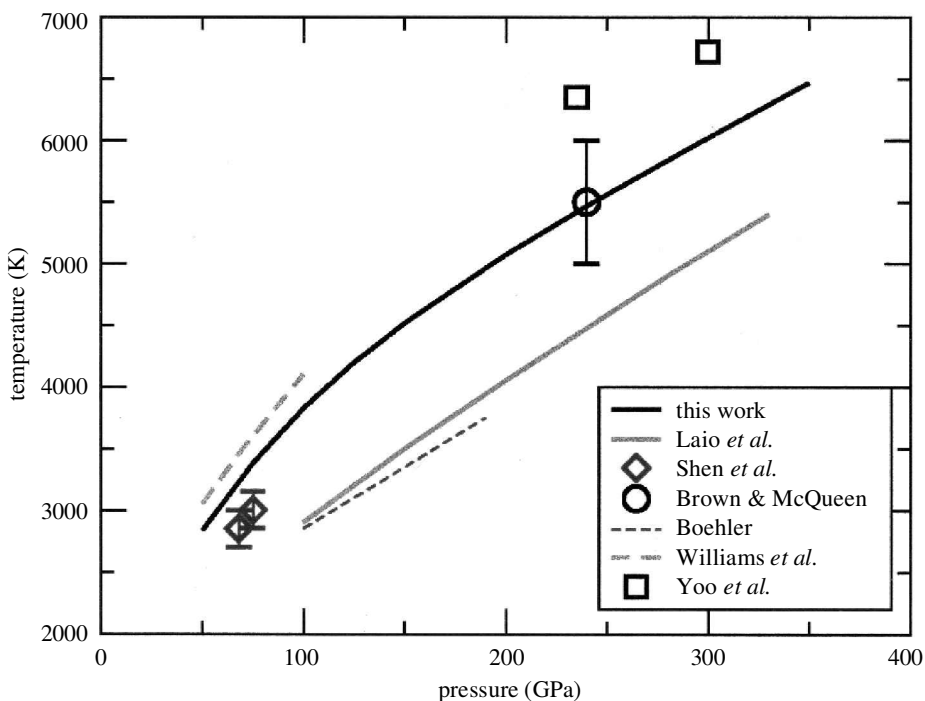


Figure 6. Our calculated high- $P$  melting curve of Fe (plotted as a solid black line) is shown passing through the shock wave datum of Brown & McQueen (1986). For comparison other experimental or calculated curves for Fe melting are also shown.

agrees almost exactly with the shock data value of Brown & McQueen (1986) and the new data of Nguyen & Holmes (1998, 2002).

There are other ways of determining the melting temperature of a system by *ab initio* methods, including performing simulations that model coexisting liquid and crystal phases. The melting temperature of this system can then be inferred by seeing which of the two phases grows during the course of a series of simulations at different temperatures. This approach has been used by Laio *et al.* (2000) and by Belonosko *et al.* (2000) to study the melting of Fe. In their study they modelled the system using interatomic potentials fitted to *ab initio* surfaces, which did not, however, simultaneously describe the liquid and crystalline phase with the same precision. We have recently also used the coexistence method, but with a model potential fitted to our own *ab initio* calculations. The raw model also fails to give the same melting temperature as obtained from our *ab initio* free-energy method, but when the results are corrected for the free energy mismatch of the model potential, the results of the two methods come into agreement. Thus it would seem as a general principle that there is a way to correct for the shortcomings of model potential coexistence calculations, namely one must calculate the free-energy differences between the model and the *ab initio* system for both the liquid and solid phases. This difference in free energy between liquid and solid can then be transformed into an effective temperature correction.

As recently highlighted by Cahn (2001), there is still scope for further work on the difficult problem of the modelling of melting, but for high- $P$  melting it appears

that there may be more problems with reconciling divergent experimental data than there are in obtaining accurate predictions of  $T_m$  from *ab initio* studies.

## 5. The composition and temperature of the core

As discussed above, on the basis of seismology and data for pure Fe it is considered that the outer and inner core contain some light element impurities. Cosmochemical abundances of the elements, combined with models of the Earth's history, limit the possible impurities to a few candidates. Those most often discussed are S, O and Si, and we have to date confined our studies to these three. Our strategy for constraining the impurity fractions and the temperature of the core is based on the supposition that the solid inner core is slowly crystallizing from the liquid outer core, and that therefore the inner and outer core are in thermodynamic equilibrium at the ICB. This implies that the chemical potentials of Fe and of each impurity must be equal on the two sides of the ICB.

If the core consisted of pure Fe, equality of the chemical potential (Gibbs free energy in this case) would tell us only that the temperature at the ICB is equal to the melting temperature of Fe at the ICB pressure of 330 GPa. With impurities present, equality of the chemical potentials for each impurity element imposes a relation between the mole fractions in the liquid and the solid, so that with S, O and Si we have three such relations. But these three relations must be consistent with the accurate values of the mass densities in the inner and outer core deduced from seismic and free-oscillation data. We outline below our recent finding (Alfè *et al.* 2002) that *ab initio* results for the densities and chemical potentials in the liquid and solid Fe/S, Fe/O and Fe/Si alloys determine with useful accuracy the mole fraction of O and the sum of the S and Si mole fractions in the outer and inner core, as well as enabling us to determine the temperature at the ICB.

The chemical potential,  $\mu_X$ , of a solute X in a solid or liquid solution is conventionally expressed as  $\mu_X = \mu_X^0 + k_B T \ln a_X$ , where  $\mu_X^0$  is a constant and  $a_X$  is the activity. It is common practice to write  $a_X = \gamma_X c_X$ , where  $\gamma_X$  is the activity coefficient and  $c_X$  the concentration of X. The chemical potential can therefore be expressed as

$$\mu_X = \mu_X^0 + k_B T \ln \gamma_X c_X, \quad (5.1)$$

which we rewrite as

$$\mu_X = \mu_X^* + k_B T \ln c_X. \quad (5.2)$$

It is helpful to focus on the quantity  $\mu_X^*$  for two reasons: first, because it is a convenient quantity to obtain by *ab initio* calculations (Alfè *et al.* 2000); second, because at low concentrations the activity coefficient,  $\gamma_X$ , will deviate only weakly from unity by an amount proportional to  $c_X$ , and by the properties of the logarithm the same will be true of  $\mu_X^*$ .

The equality of the chemical potentials  $\mu_X^l$  and  $\mu_X^s$  in coexisting liquid and solid (superscripts 'l' and 's', respectively) then requires that

$$\mu_X^{*l} + k_B T \ln c_X^l = \mu_X^{*s} + k_B T \ln c_X^s, \quad (5.3)$$

or, equivalently,

$$\frac{c_X^s}{c_X^l} = \exp \left[ \frac{\mu_X^{*l} - \mu_X^{*s}}{k_B T} \right]. \quad (5.4)$$

This means that the ratio of the mole fractions  $c_X^s$  and  $c_X^l$  in the solid and liquid solution is determined by the liquid and solid thermodynamic quantities  $\mu_X^{*l}$  and  $\mu_X^{*s}$ . Although liquid–solid equilibrium in the Fe/S and Fe/O systems has been experimentally studied up to pressures of *ca.* 60 GPa, there seems little prospect of obtaining experimental data for  $\mu_X^{*l} - \mu_X^{*s}$  for Fe alloys at the much higher ICB pressure. However, we have shown (Alfè *et al.* 2000) recently that the fully *ab initio* calculation of  $\mu_X^{*l}$  and  $\mu_X^{*s}$  is technically feasible. Thus, the chemical potential,  $\mu_X$ , of chemical component X can be defined as the change of Helmholtz free energy when one atom of X is introduced into the system at constant temperature  $T$  and volume  $V$ . In *ab initio* simulations, it is awkward to introduce a new atom, but the awkwardness can be avoided by calculating  $\mu_X^* - \mu_{\text{Fe}}^*$ , which is the free-energy change,  $\Delta F$ , when an Fe atom is replaced by an X atom. For the liquid, this  $\Delta F$  is computed by applying the technique of ‘thermodynamic integration’ to the (hypothetical) process in which an Fe atom is continuously transmuted into an X atom. We have recently performed such calculations for transmuting Fe atoms into S, O and Si (Alfè *et al.* 2002).

The full technical details of our simulations are given in Alfè *et al.* (2000, 2002), but in brief, they were performed at constant volume and temperature on systems of 64 atoms; the duration of the simulations after equilibration was typically 6 ps in order to reduce statistical errors to an acceptable level; the number of thermodynamic integration points used in transmuting Fe into X was three, and we carefully checked the adequacy of these numbers of points. Our results reveal a major qualitative difference between O and the other two impurities. For S and Si,  $\mu_X^*$  is almost the same in the solid and the liquid, the differences being at most 0.3 eV, i.e. markedly smaller than  $k_B T \approx 0.5$  eV; but for O the difference of  $\mu_X^*$  between solid and liquid is *ca.* 2.6 eV, which is much bigger than  $k_B T$ . This means that added O will partition strongly into the liquid, but added S or Si will have similar concentrations in the two phases.

Our simulations of the chemical potentials of the alloys can be combined with simulations of their densities to investigate whether the known densities of the liquid and solid core can be matched by any binary Fe/X system, with X = S, O or Si. Using our calculated partial volumes of S, Si and O in the binary liquid alloys, we find that the mole fractions required to reproduce the liquid core density are 16, 14 and 18% respectively (figure 7a displays our predicted liquid density as a function of  $c_X$  compared with the seismic density). Our calculated chemical potentials in the binary liquid and solid alloys then give the mole fractions in the solid of 14, 14 and 0.2%, respectively, that would be in equilibrium with these liquids (see figure 7b). Finally, our partial volumes in the binary solids give ICB density discontinuities of  $2.7 \pm 0.5$ ,  $1.8 \pm 0.5$  and  $7.8 \pm 0.2\%$ , respectively (figure 7c). As expected, for S and Si, the discontinuities are considerably smaller than the known value of  $4.5 \pm 0.5\%$ ; for O, the discontinuity is markedly greater than the known value. We conclude that none of the binary systems can account for the discontinuity quantitatively. However, it clearly can be accounted for by O together with either or both of S and Si. *Ab initio* calculations on general quaternary alloys containing Fe, S, O and Si will clearly be feasible in the future, but currently they are computationally too demanding, so for the moment we assume that the chemical potential of each impurity species is unaffected by the presence of the others. Our estimated mole fractions needed to account for the ICB density discontinuity, reported in table 1, show that we must have *ca.* 8% of O in the outer core and a slightly larger amount of S and/or Si.

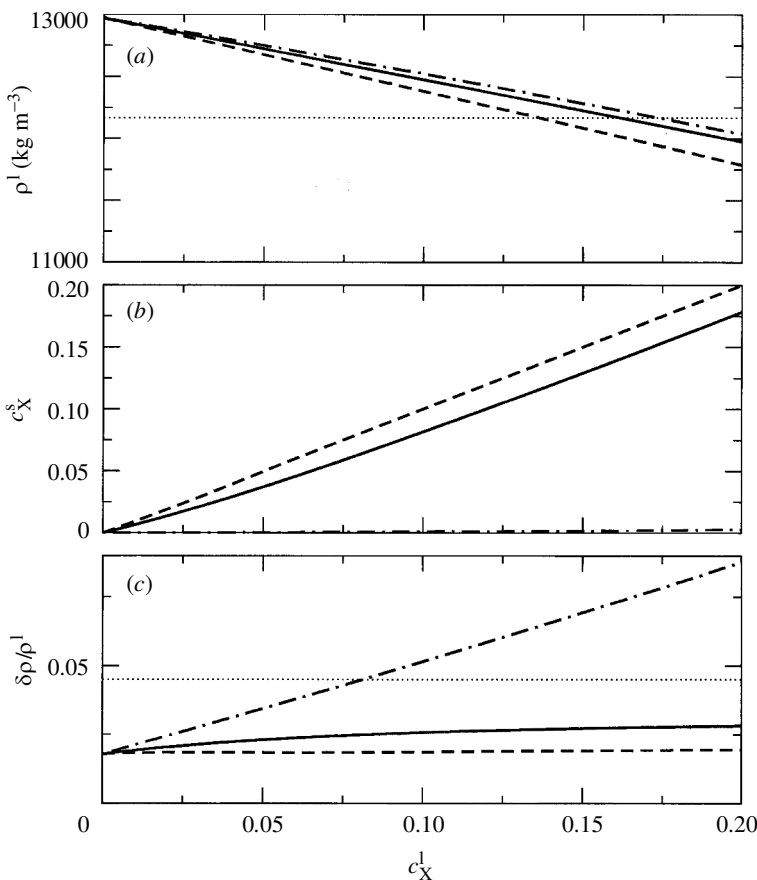


Figure 7. Liquid and solid impurity mole fractions  $c_X^l$  and  $c_X^s$  of impurities X = S, Si and O, and resulting densities of the inner and outer core predicted by *ab initio* simulations. Solid, dashed and chain curves represent S, Si and O, respectively. (a) Liquid density  $\rho^l$  ( $\text{kg m}^{-3}$ ); horizontal dotted line shows density from seismic data. (b) Mole fractions in solid resulting from equality of chemical potentials in solid and liquid. (c) Relative density discontinuity ( $\delta\rho/\rho^l$ ) at the ICB; horizontal dotted line is the value from free oscillation data.

Table 1. Estimated molar percentages

(Estimated molar percentages of sulphur, silicon and oxygen in the solid inner core and liquid outer core obtained by combining *ab initio* calculations and seismic data. Sulphur/silicon entries refer to total percentages of sulphur and/or silicon.)

	solid	liquid
sulphur/silicon	$8.5 \pm 2.5$	$10.0 \pm 2.5$
oxygen	$0.2 \pm 0.1$	$8.0 \pm 2.5$

With our calculated impurity chemical potentials, we used the Gibbs–Duhem relation to compute the change in the Fe chemical potential caused by the impurities in the solid and liquid phases (Alfè *et al.* 2002). By requiring the chemical potential of Fe to be the same in both phases, we obtained the change,  $\Delta T$ , of melting

temperature relative to that of pure Fe. Our estimate is  $\Delta T = -700 \pm 100$  K. Using our own *ab initio* estimate of the melting temperature of pure Fe at a core pressure of 6200–6350 K, we predict that the Earth's temperature at the ICB is *ca.* 5600 K. Interestingly, this is very close to the value recently inferred by Steinle-Neumann *et al.* (2001) from independently determined *ab initio* calculations on the elastic properties of the inner core and to the value inferred by Poirier & Shankland (1993) from dislocation melting theory.

## 6. Conclusion

The past decade has seen a major advance in the application of *ab initio* methods in the solution of high-pressure and temperature geophysical problems, thanks to the rapid developments in high-performance computing. We are now in a position to calculate from first principles the free energies of solid and liquid phases, and hence to determine both the phase relations and the physical properties of planetary forming phases. Our work suggests that the inner core of the Earth is composed of HCP-Fe containing *ca.* 8.5% S (or Si) and 0.2% O in equilibrium at 5600 K at the ICB with a liquid Fe outer core containing *ca.* 10% S (or Si) and 8% O.

In the future, we look forward to the advent of routinely available ‘terascale’ computing. This will open new possibilities for geophysical modelling. Thus, we will be able to model more complex and larger systems, to investigate for example solid-state rheological problems, or physical properties such as thermal and electrical conductivity. Furthermore, however, we recognize that the DFT methods we currently use are still approximate, and fail for example to describe the band structure of important phases such as FeO. In the future we intend to use terascale facilities to implement more demanding but more accurate techniques, such as those based on quantum Monte Carlo methods.

D.A., J.B. and L.V. are supported by Royal Society University Research Fellowships. M.J.G. thanks GEC and Daresbury Laboratory for their support. This work was supported by NERC grants GR3/12083 and GR9/03550. The calculations were run on the Cray T3D and Cray T3E machines at Edinburgh and the Manchester CSAR Centre and on the Origin 2000 machine at the UCL HiPerSPACE Centre.

## References

- Alfè, D. 1999 *Ab initio* molecular dynamics, a simple algorithm for charge extrapolation. *Comput. Phys. Commun.* **118**, 31–33.
- Alfè, D., Gillan, M. J. & Price, G. D. 1999 The melting curve of iron at the pressures of the Earth's core from *ab initio* calculations. *Nature* **401**, 462–464.
- Alfè, D., Gillan, M. J. & Price, G. D. 2000 Constraints on the composition of the Earth's core from *ab initio* calculations. *Nature* **405**, 172–175.
- Alfè, D., Gillan, M. J. & Price, G. D. 2002 Composition and temperature of the Earth's core constrained by combining *ab initio* calculations and seismic data. *Earth Planet. Sci. Lett.* **195**, 91–98.
- Allen, M. P. & Tildesley, D. J. 1987 *Computer simulation of liquids*. Oxford University Press.
- Anderson, O. L. 1995 *Equations of state of solids for geophysics and ceramic science*. Oxford University Press.
- Andrault, D., Fiquet, G., Kunz, M., Visocikas, F. & Häusermann, D. 1997 The orthorhombic structure of iron: an *in situ* study at high temperature and high pressure. *Science* **278**, 831–834.

- Belonosko, A. B., Ahuja, R. & Johansson, B. 2000 Quasi-*ab initio* molecular dynamic study of Fe melting. *Phys. Rev. Lett.* **84**, 3638–3641.
- Birch, F. 1964 Density and composition of mantle and core. *J. Geophys. Res.* **69**, 4377–4388.
- Boehler, R. 1993 Temperature in the Earth's core from the melting point measurements of iron at high static pressures. *Nature* **363**, 534–536.
- Born, M. & Huang, K. 1954 *Dynamical theory of crystal lattices*. Oxford University Press.
- Brown, J. M. & McQueen, R. G. 1986 Phase transitions, Grüneisen parameter and elasticity for shocked iron between 77 GPa and 400 GPa. *J. Geophys. Res.* **91**, 7485–7494.
- Cahn, R. W. 2001 Melting from within. *Nature* **413**, 582–583.
- Car, R. & Parrinello, M. 1985 Unified approach for molecular dynamics and density functional theory. *Phys. Rev. Lett.* **55**, 2471–2474.
- Cohen, M. & Heine, V. 1970 The fitting of pseudopotentials to experimental data and their subsequent application. In *Solid state physics* (ed. H. Ehrenreich, F. Seitz & D. Turnbull), vol. 24, pp. 237–248.
- de Wijs, G. A., Kresse, G., Gillan, M. J. & Price, G. D. 1998 First-order phase transitions by first principles free-energy calculations: the melting of Al. *Phys. Rev. B* **57**, 8233–8234.
- Gao, F., Johnston, R. L. & Murrell, J. N. 1993 Empirical many-body potential energy functions for iron. *J. Phys. Chem.* **97**, 12 073–12 082.
- Gillan, M. J. 1997 The virtual matter laboratory. *Contemp. Phys.* **38**, 115–130.
- Heine, V. 1970 The pseudopotential concept. In *Solid state physics* (ed. H. Ehrenreich, F. Seitz & D. Turnbull), vol. 24, pp. 1–36.
- Heine, V. & Weaire, D. 1970 Pseudopotential theory of cohesion and structure. In *Solid state physics* (ed. H. Ehrenreich, F. Seitz & D. Turnbull), vol. 24, pp. 249–463.
- Hohenberg, P. & Kohn, W. 1964 Inhomogeneous electron gas. *Phys. Rev. B* **136**, 864–871.
- Kohn, W. & Sham, L. J. 1965 Self consistent equations including exchange and correlation effects. *Phys. Rev. A* **140**, 1133–1138.
- Kresse, G. & Furthmüller, J. 1996 Efficient iterative schemes for *ab initio* total-energy calculations using a plane-wave basis set. *Phys. Rev. B* **54**, 11 169–11 186.
- Kresse, G., Furthmüller, J. & Hafner, J. 1995 *Ab initio* force-constant approach to phonon dispersion relations of diamond and graphite. *Europhys. Lett.* **32**, 729–734.
- Laio, A., Bernard, S., Chiarotti, G. L., Scandolo, S. & Tosatti, E. 2000 Physics of iron at Earth's core conditions. *Science* **287**, 1027–1030.
- Matsui, M. & Anderson, O. L. 1997 The case for a body-centered cubic phase for iron at inner core conditions. *Phys. Earth Planet. Inter.* **103**, 55–62.
- Matsui, M., Price, G. D. & Patel, A. 1994 Comparison between the lattice dynamics and molecular dynamics methods: calculation results for MgSiO<sub>3</sub> Perovskite. *Geophys. Res. Lett.* **21**, 1659–1662.
- Nguyen, J. H. & Holmes, N. C. 1998 Iron sound velocities in shock wave experiments up to 400 GPa. *Eos* (abstracts) **79**, T21D-06.
- Nguyen, J. H. & Holmes, N. C. 2002 Iron sound velocity and its implications for the iron phase diagram. *Science*. (In the press.)
- Parker, S. C. & Price, G. D. 1989 Computer modelling of phase transitions in minerals. *Adv. Solid State Chem.* **1**, 295–327.
- Parrinello, M. & Rahman, A. 1980 Crystal structure and pair potentials: a molecular dynamics study. *Phys. Rev. Lett.* **45**, 1196–1199.
- Poirier, J. P. 1994 Light elements in the Earth's outer core: a critical review. *Phys. Earth Planet. Inter.* **85**, 319–337.
- Poirier, J. P. & Shankland, T. J. 1993 Dislocation melting of iron and the temperature of the inner ice core boundary, revisited. *Geophys. J. Int.* **115**, 147–151.

- Pulay, P. 1980 Convergence acceleration of iterative sequences. The case of SCF iteration. *Chem. Phys. Lett.* **73**, 393.
- Saxena, S. K., Dubrovinsky, L. S. & Häggkvist, P. 1996 X-ray evidence for the new phase of  $\bar{\alpha}$ -iron at high temperature and high pressure. *Geophys. Res. Lett.* **23**, 2441–2444.
- Shen, G. Y., Mao, H. K., Hemley, R. J., Duffy, T. S. & Rivers, M. L. 1998 Melting and crystal structure of iron at high pressures and temperatures. *Geophys. Res. Lett.* **25**, 373.
- Söderlind, P., Moriarty, J. A. & Wills, J. M. 1996 First-principles theory of iron up to earth-core pressures: structural, vibrational and elastic properties. *Phys. Rev. B* **53**, 14 063–14 072.
- Steinle-Neumann, G., Stixrude, L., Cohen, R. E. & Gülsen, O. 2001 Elasticity of iron at the temperature of the Earth's inner core. *Nature* **413**, 57–60.
- Stixrude, L. & Cohen, R. E. 1995 Constraints on the crystalline structure of the inner core—mechanical instability of BCC iron at high-pressure. *Geophys. Res. Lett.* **22**, 125–128.
- Stixrude, L., Wasserman, E. & Cohen, R. E. 1997 Composition and temperature of the Earth's inner core. *J. Geophys. Res.* **102**, 24 729–24 739.
- Vočadlo, L. & Alfè, D. 2002 The *ab initio* melting curve of aluminium. *Phys. Rev. B*. (In the press.)
- Vočadlo, L., Brodholt, J., Alfè, D., Price, G. D. & Gillan, M. J. 1999 The structure of iron under the conditions of the Earth's inner core. *Geophys. Res. Lett.* **26**, 1231–1234.
- Wallace, D. C. 1998 *Thermodynamics of crystals*. New York: Dover.
- Wang, Y. & Perdew, J. P. 1991 Correlation hole of the spin-polarized electron-gas, with exact small-wave-vector and high-density scaling. *Phys. Rev. B* **44**, 13 298–13 307.
- Wasserman, E., Stixrude, L. & Cohen, R. E. 1996 Thermal properties of iron at high pressures and temperatures. *Phys. Rev. B* **53**, 8296–8309.
- Yoo, C. S., Holmes, N. C., Ross, M., Webb, D. J. & Pike, C. 1993 Shock temperatures and melting of iron at Earth core conditions. *Phys. Rev. Lett.* **70**, 3931–3934.